37. FRAGMENTATION FUNCTIONS IN e^+e^- ANNIHILATION

Written September 2001 by O. Biebel (Max-Planck-Institut für Physik, Munich, Germany), P. Nason (INFN, Sez. di Milano, Milan, Italy), and B.R. Webber (Cavendish Laboratory, Cambridge, UK). An extended version of this review can be found in Ref. 1

37.1. Introduction

Fragmentation functions are dimensionless functions that describe the final-state single-particle energy distributions in hard scattering processes. The total e^+e^- fragmentation function for hadrons of type h in annihilation at c.m. energy $\sqrt{s}$, via an intermediate vector boson $V = \gamma/Z^0$, is defined as

$$F^h(x,s) = \frac{1}{\sigma_{\rm tot}}\frac{d\sigma}{dx}(e^+e^- \to V \to hX) \tag{37.1}$$

where $x = 2E_h/\sqrt{s} \le 1$ is the scaled hadron energy (in practice, the approximation $x = x_p = 2p_h/\sqrt{s}$ is often used). Its integral with respect to x gives the average multiplicity of those hadrons:

$$\langle n_h(s)\rangle = \int_0^1 dx\, F^h(x,s)\ . \tag{37.2}$$

Neglecting contributions suppressed by inverse powers of s, the fragmentation function (37.1) can be represented as a sum of contributions from the different parton types $i = u, \overline{u}, d, \overline{d}, \ldots, g$:

$$F^h(x,s) = \sum_i \int_x^1 \frac{dz}{z} C_i(s;z,\alpha_{\rm S}) D_i^h(x/z,s)\ . \tag{37.3}$$

where D_i^h are the parton fragmentation functions. At lowest order in $\alpha_{\rm S}$ the coefficient function C_g for gluons is zero, while for quarks $C_i = g_i(s)\delta(1-z)$ where $g_i(s)$ is the appropriate electroweak coupling. In particular, $g_i(s)$ is proportional to the charge-squared of parton i at $s \ll M_Z^2$, when weak effects can be neglected. In higher orders the coefficient functions and parton fragmentation functions are factorization-scheme dependent.

Parton fragmentation functions are analogous to the parton distributions in deep inelastic scattering (see sections on QCD and Stucture Functions (9 and 36 of this *Review*). In both cases, the simplest parton-model approach would predict a scale-independent x distribution. Furthermore we obtain similar violations of this scaling behaviour when QCD corrections are taken into account.

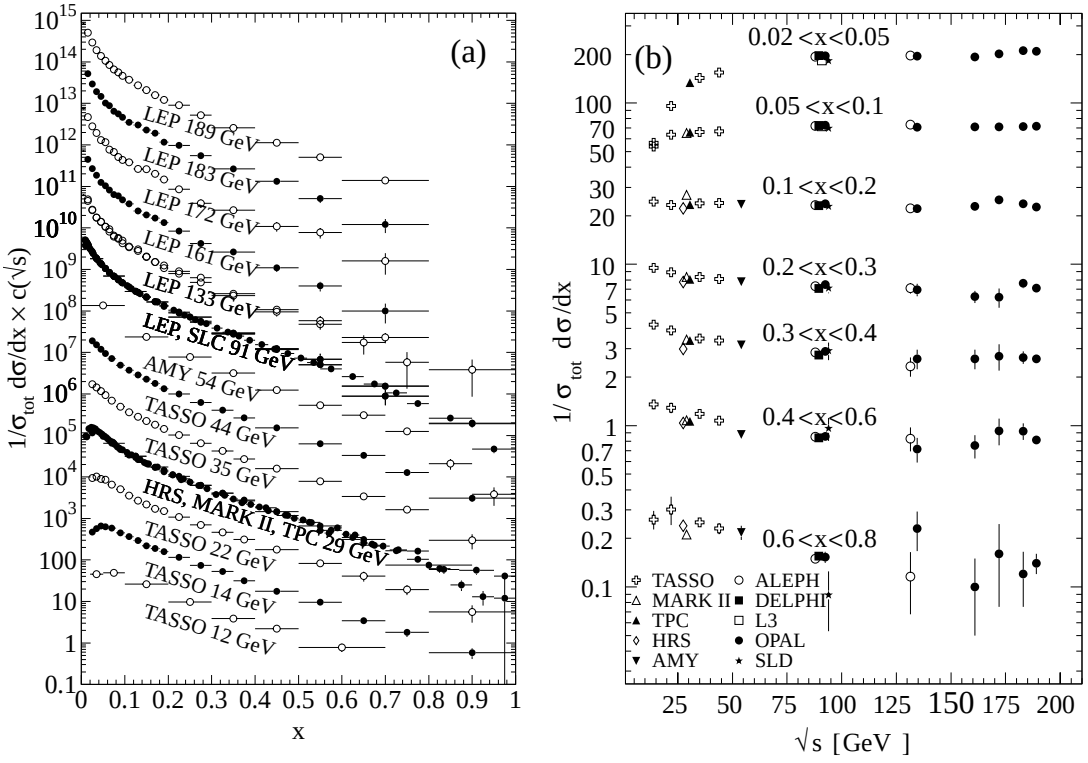

Figure 37.1: The e^+e^- fragmentation function for all charged particles is shown [6,7,8,9](a) for different c.m. energies, $\sqrt{s}$, versus x and (b) for various ranges of x versus $\sqrt{s}$. For the purpose of plotting (a), the distributions were scaled by $c(\sqrt{s}) = 10^i$ where i is ranging from $i = 0$ ($\sqrt{s} = 12$ GeV) to $i = 12$ ($\sqrt{s} = 189$ GeV).

37.2. Scaling violation

The evolution of the parton fragmentation function $D_i(x,t)$ with increasing scale $t = s$, like that of the parton distribution function $f_i(x,t)$ with $t = s$ (see Sec. 35 of this *Review*), is governed by the DGLAP equation [2]

$$t\frac{\partial}{\partial t}D_i(x,t) = \sum_j \int_x^1 \frac{dz}{z}\frac{\alpha_S}{2\pi}P_{ji}(z,\alpha_S)D_j(x/z,t)\ . \tag{37.4}$$

In analogy to DIS, in some cases an evolution equation for the fragmentation function F itself (Eq. (37.3)) can be derived from Eq. (37.4) [3]. Notice that the splitting function is now P_{ji} rather than P_{ij} since here D_j represents the fragmentation of the final parton. The splitting functions again have perturbative expansions of the form

$$P_{ji}(z,\alpha_S) = P_{ji}^{(0)}(z) + \frac{\alpha_S}{2\pi}P_{ji}^{(1)}(z) + \cdots \tag{37.5}$$

where the lowest-order functions $P_{ji}^{(0)}(z)$ are the same as those in deep inelastic scattering but the higher-order terms [4] [1] are different. The effect of evolution is, however, the same in both cases: as the scale increases, one observes a scaling violation in which the x distribution is shifted towards lower values. This can be seen from Fig. 37.1.

The coefficient functions C_i in Eq. (37.3) and the splitting functions P_{ji} contain singularities at $z = 0$ and 1, which have important effects on fragmentation at small and large values of x, respectively. For details see *e.g.*, Ref. 1.

Quantitative results of studies of scaling violation in e^+e^- fragmentation are reported in Refs. 10,12. The values of α_S obtained are consistent with the world average (see section on QCD in Sec. 9 of this *Review*).

37.3. Longitudinal Fragmentation

In the process $e^+e^- \to V \to hX$, the joint distribution in the energy fraction x and the angle θ between the observed hadron h and the incoming electron beam has the general form

$$\frac{1}{\sigma_{\rm tot}}\frac{d^2\sigma}{dx\, d\cos\theta} = \frac{3}{8}(1+\cos^2\theta)\,F_T(x) + \frac{3}{4}\sin^2\theta\,F_L(x) + \frac{3}{4}\cos\theta\,F_A(x)\ , \qquad (37.6)$$

where F_T, F_L and F_A are respectively the transverse, longitudinal and asymmetric fragmentation functions. All these functions also depend on the c.m. energy $\sqrt{s}$. Eq. (37.6) is the most general form of the inclusive single particle production from the decay of a massive vector boson [3]. As their names imply, F_T and F_L represent the contributions from virtual bosons polarized transversely or longitudinally with respect to the direction of motion of the hadron h. F_A is a parity-violating contribution which comes from the interference between vector and axial vector contributions. Integrating over all angles, we obtain the total fragmentation function, $F = F_T + F_L$. Each of these functions can be represented as a convolution of the parton fragmentation functions D_i with appropriate coefficient functions $C_i^{\rm T,L,A}$ as in Eq. (37.3). This representation works in the high energy limit. As $x \cdot \sqrt{s}/2$ approaches hadronic scales $\simeq m_\rho$, power suppressed effects can no longer be neglected, and the fragmentation function formalism no longer accounts correctly for the separation of F_T, F_L, and F_A. In Fig. 37.2, F_T, F_L, and F_A measured at $\sqrt{s} = 91$ GeV are shown.

[1] There are misprints in the formulae in the published article. The correct expressions can be found in the preprint version or in Ref. 5.

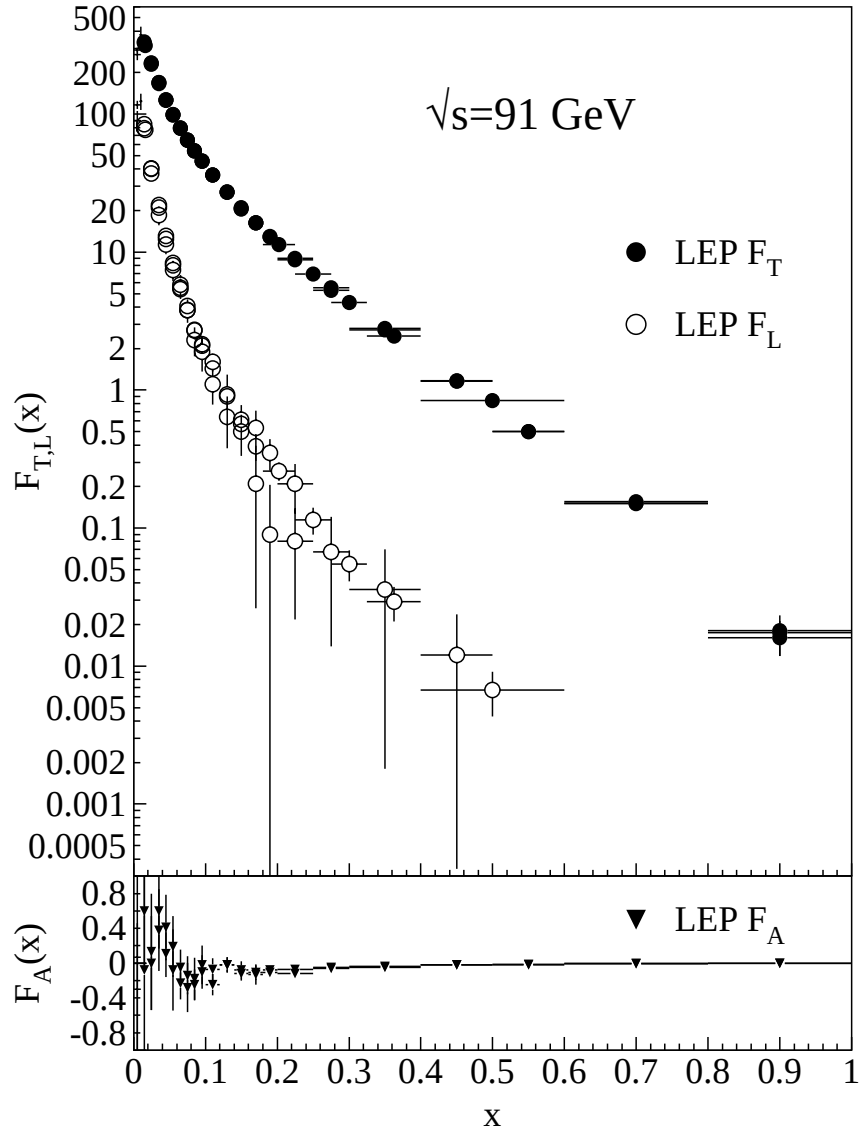

Figure 37.2: Transverse (F_T), longitudinal (F_L), and asymmetric (F_A) fragmentation functions are shown [8,11,13]. Data points with relative errors greater than 100% are omitted.

37.4. Gluon fragmentation

The gluon fragmentation function $D_g(x)$ can be extracted from the longitudinal fragmentation function defined in Eq. (37.6). Since the coefficient functions $C_i^{\rm L}$ for quarks and gluons are comparable in $\mathcal{O}(\alpha_{\rm S})$, F_L can be expressed in terms of F_T and D_g which

allows one to obtain D_g from the measured F_L and F_T. It can also be deduced from the fragmentation of three-jet events in which the gluon jet is identified, for example by tagging the other two jets with heavy quark decays. To leading order the measured distributions of $x = E_{\rm had}/E_{\rm jet}$ for particles in gluon jets can be identified directly with the gluon fragmentation functions $D_g(x)$. The experimentally measured gluon fragmentation functions are shown in Fig. 37.3.

37.5. Fragmentation models

Although the scaling violation can be calculated perturbatively, the actual form of the parton fragmentation functions is non-perturbative. Perturbative evolution gives rise to a shower of quarks and gluons (partons). Phenomenological schemes are then used to model the carry-over of parton momenta and flavour to the hadrons. Two of the very popular models are the *string fragmentation* [15,16], implemented in the JETSET [17] and UCLA [18] Monte Carlo event generation programs, and the *cluster fragmentation* of the HERWIG Monte Carlo event generator [19].

37.5.1. ***String fragmentation***: The string-fragmentation scheme considers the colour field between the partons, *i.e.*, quarks and gluons, to be the fragmenting entity rather than the partons themselves. The string can be viewed as a colour flux tube formed by gluon self-interaction as two coloured partons move apart. Energetic gluon emission is regarded as energy-momentum carrying "kinks" on the string. When the energy stored in the string is sufficient, a $q\overline{q}$ pair may be created from the vacuum. Thus the string breaks up repeatedly into colour singlet systems as long as the invariant mass of the string pieces exceeds the on-shell mass of a hadron. The $q\overline{q}$ pairs are created according to the probability of a tunnelling process $\exp(-\pi m^2_{q,\perp}/\kappa)$ which depends on the transverse mass squared $m^2_{q,\perp} \equiv m^2_q + p^2_{q,\perp}$ and the string tension $\kappa \approx 1$ GeV/fm. The transverse momentum $p_{q,\perp}$ is locally compensated between quark and antiquark. Due to the dependence on the parton mass m_q and/or hadron mass, m_h, the production of strange and, in particular, heavy-quark hadrons is suppressed. The light-cone momentum fraction $z = (E + p_\parallel)_h/(E + p)_q$, where $p_\parallel$ is the momentum of the formed hadron h along the direction of the quark q, is given by the string-fragmentation function

$$f(z) \sim \frac{1}{z}(1-z)^a \exp\left(-\frac{bm^2_{h,\perp}}{z}\right) \tag{37.7}$$

where a and b are free parameters. These parameters need to be adjusted to bring the fragmentation into accordance with measured data, *e.g.*, $a = 0.11$ and $b = 0.52$ GeV^{-2} as determined in Ref. 20 (for an overview on tuned parameters see Ref. 21).

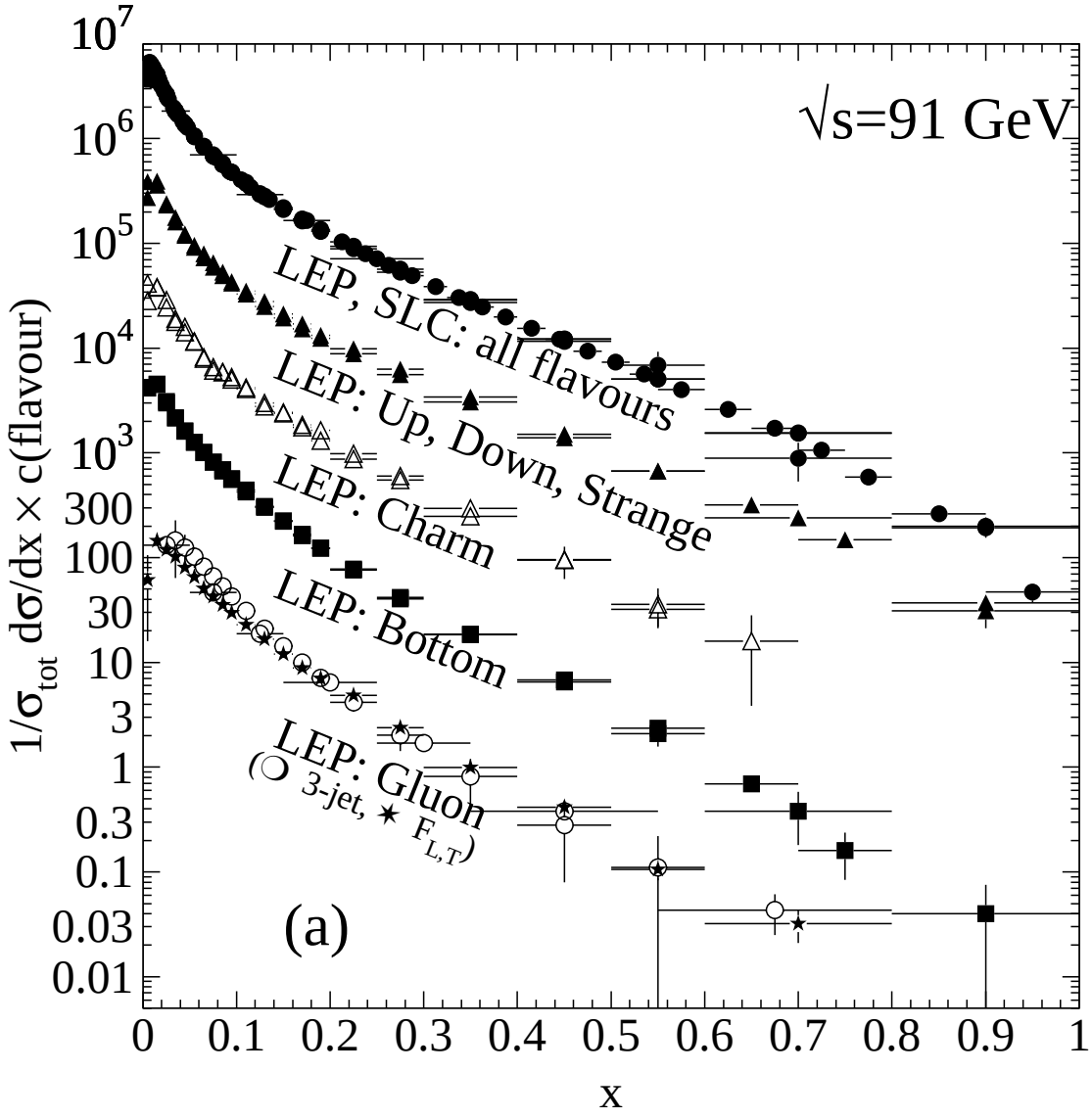

Figure 37.3: Comparison of the charged-particle and the flavour-dependent e^+e^- fragmentation functions obtained at $\sqrt{s} = 91$ GeV. The data [8,9,10,13,14] are shown for the inclusive, light (up, down, strange) quarks, charm quark, bottom quark, and the gluon versus x. For the purpose of plotting, the distributions were scaled by c(flavour) $= 10^i$ where i is ranging from $i = 0$ (Gluon) to $i = 4$ (all flavours).

37.5.2. ***Cluster fragmentation***: Assuming a local compensation of colour based on the *pre-confinement* property of perturbative QCD [22], the remaining gluons at the end of the parton shower evolution are split non-perturbatively into quark-antiquark pairs. Colour singlet clusters of typical mass of a couple of GeV are then formed from quark and antiquark of colour-connected splittings. These clusters decay directly into two hadrons unless they are either too heavy (relative to an adjustable parameter `CLMAX`, default value 3.35 GeV), when they decay into two clusters, or too light, in which case a cluster decays into a single hadron, requiring a small rearrangement of energy and momentum with neighbouring clusters. The decay of a cluster into two hadrons is assumed to be isotropic in the rest frame of the cluster except if a perturbative-formed quark is involved. A decay channel is chosen based on the phase-space probability, the density of states, and the spin degeneracy of the hadrons. Cluster fragmentation has a compact description with few parameters, due to the phase-space dominance in the hadron formation.

37.6. Experimental studies

A great wealth of measurements of e^+e^- fragmentation into identified particles exists. A collection of references to find data on the fragmentation into identified particles is given for Table 38.1. As representatives of all the data, Fig. 37.4 shows fragmentation functions as the scaled momentum spectra of charged particles at several c.m. energies. Heavy flavour particles are dealt with separately in Sec. 37.7.

The measured fragmentation functions are solutions to the DGLAP equation (37.4) but need to be parametrized at some initial scale t_0 (usually 2 GeV^2 for light quarks and gluons). A general parametrization is [24]

$$D_{p\to h}(x,t_0) = Nx^\alpha(1-x)^\beta\left(1+\frac{\gamma}{x}\right) \tag{37.8}$$

where the normalization N, and the parameters α, β, and γ in general depend on the energy scale t_0 and also on the type of the parton, p, and the hadron, h. Frequently the term involving γ is left out [25]. The parameters of Eq. (37.8), listed in Ref. 25, were obtained by fitting data on various hadron types for different combinations of partons and hadrons in $p \to h$ in the range $\sqrt{s} \approx$ 5–200 GeV.

37.7. Heavy quark fragmentation

It was recognized very early [26] that a heavy flavoured meson should retain a large fraction of the momentum of the primordial heavy quark, and therefore its fragmentation function should be much harder than that of a light hadron. In the limit of a very heavy quark, one expects the fragmentation function for a heavy quark to go into any heavy hadron to be peaked near 1.

When the heavy quark is produced at a momentum much larger than its mass, one expects important perturbative effects, enhanced by powers of the logarithm of the transverse momentum over the heavy quark mass, to intervene and modify the shape of the fragmentation function. In leading logarithmic order (*i.e.*, including all powers of $\alpha_S \log m_Q/p_T$) the total (*i.e.*, summed over all hadron types) perturbative

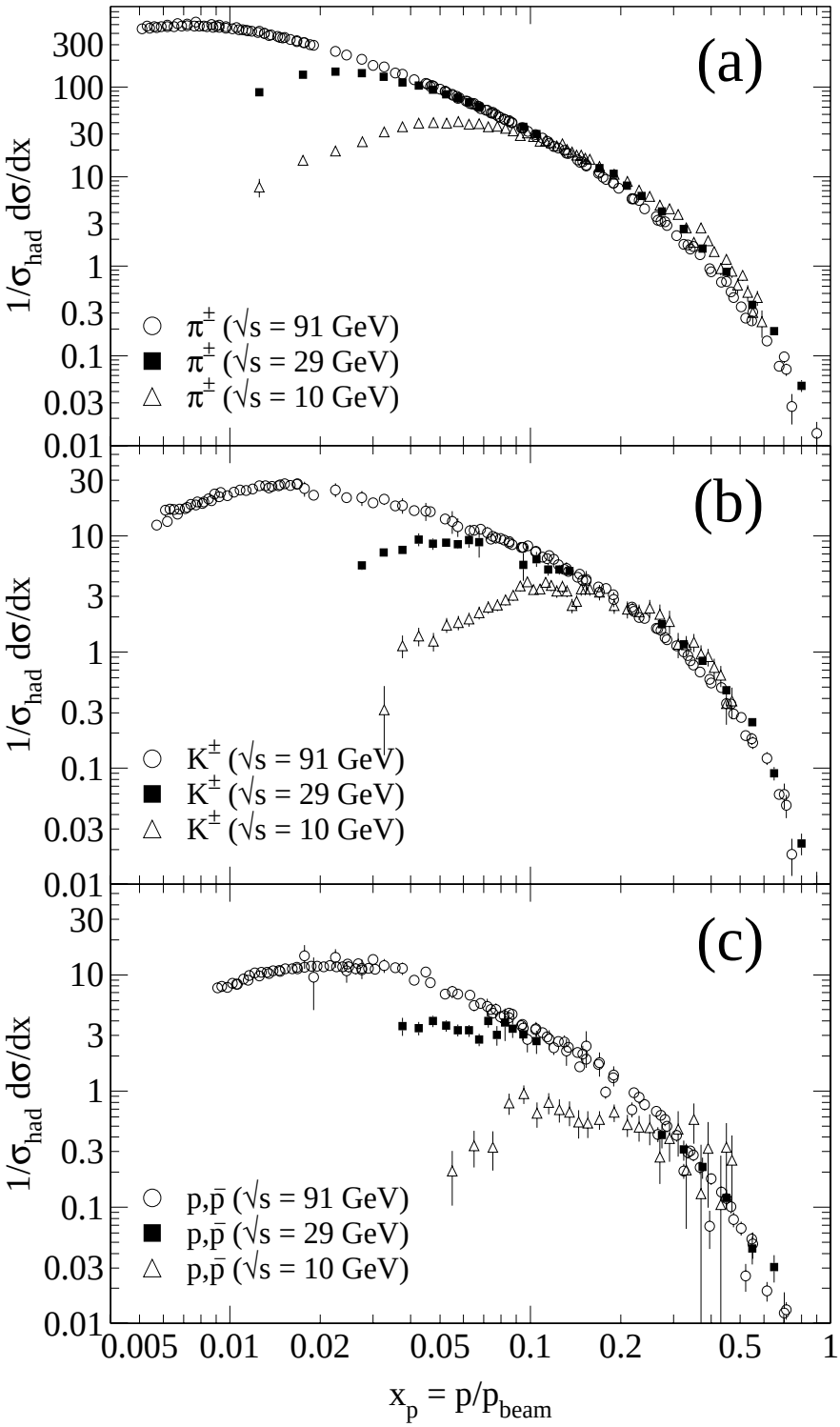

Figure 37.4: Scaled momentum spectra of (a) $\pi^\pm$, (b) $K^\pm$, and (c) $p/\overline{p}$ at $\sqrt{s} = 10$, 29, and 91 GeV are shown [7,23].

fragmentation function is simply obtained by solving the leading evolution equation for fragmentation functions, Eq. (37.4), with the initial condition at a scale $\mu^2 = m_{\rm Q}^2$ given by $D_{\rm Q}(z, m_{\rm Q}^2) = \delta(1-z)$ and $D_i(z, m_{\rm Q}^2) = 0$ for $i \neq {\rm Q}$ (the notation $D_i(z)$ stands for the probability to produce a heavy quark Q from parton i with a fraction z of the parton momentum).

Several extensions of the leading logarithmic result have appeared in the literature. Next-to-leading-log (NLL) order results for the perturbative heavy quark fragmentation function have been obtained in Ref. 27. At large z, phase space for gluon radiation is suppressed. This exposes large perturbative corrections due to the incomplete cancellation of real gluon radiation and virtual gluon exchange (Sudakov effects), which should be resummed in order to get accurate results. A leading-log (LL) resummation formula has been obtained in Refs. 27,28. Next-to-leading-log resummation has been performed in Ref. 29. Fixed-order calculations of the fragmentation function at order $\alpha_{\rm S}^2$ in e^+e^- annihilation have appeared in Ref. 30. This result does not include terms of order $(\alpha_{\rm S} \log s/m^2)^k$ and $\alpha_{\rm S}(\alpha_{\rm S} \log s/m^2)^k$, but it does include correctly all terms up to the order $\alpha_{\rm S}^2$, including terms without any logarithmic enhancements.

Inclusion of non-perturbative effects in the calculation of the heavy quark fragmentation function is done in practice by convolving the perturbative result with a phenomenological non-perturbative form. Among the most popular parametrizations we have the following:

$$\text{Peterson } \textit{et al.} \quad [3]: \qquad D_{\rm np}(z) \propto \frac{1}{z}\left(1 - \frac{1}{z} - \frac{\epsilon}{1-z}\right)^{-2}, \tag{37.9}$$

$$\text{Kartvelishvili } \textit{et al.} \quad [32]: \qquad D_{\rm np}(z) \propto z^{\alpha}(1-z), \tag{37.10}$$

$$\text{Collins\&Spiller} \quad [33]: \qquad D_{\rm np}(z) \propto \left(\frac{1-z}{z} + \frac{(2-z)\epsilon_C}{1-z}\right) \times (1+z^2)\left(1 - \frac{1}{z} - \frac{\epsilon_C}{1-z}\right)^{-2} \tag{37.11}$$

where ϵ, α, and ϵ_C are non-perturbative parameters, depending upon the heavy hadron considered. In general, the non-perturbative parameters do not have an absolute meaning. They are fitted together with some model of hard radiation, which can be either a shower Monte Carlo, a leading-log or NLL calculation (which may or may not include Sudakov resummation), or a fixed order calculation. In Ref. 30, for example, the ϵ parameter for charm and bottom production is fitted from the measured distributions of Refs. 34,35 for charm, and of Ref. 36 for bottom. If the leading-logarithmic approximation (LLA) is used for the perturbative part, one finds $\epsilon_c \approx 0.05$ and $\epsilon_b \approx 0.006$; if a second order calculation is used one finds $\epsilon_c \approx 0.035$ and $\epsilon_b \approx 0.0033$; if a NLLO calculation is used instead one finds $\epsilon_c \approx 0.022$ and $\epsilon_b \approx 0.0023$. The larger values found in the LL approximation are consistent with what is obtained in the context of parton shower models [37], as expected. The ϵ parameter for charm and bottom scales roughly with the inverse square of the heavy flavour mass. This behaviour can be justified by several arguments [26,38]. It can be used to relate the non-perturbative parts of the fragmentation functions of charm and bottom quarks [30,39].

The bulk of the available fragmentation function data on charmed mesons (excluding $J/\psi(1S)$) is from measurements in e^+e^- annihilation at $\sqrt{s} \approx 10$ GeV. Shown in Fig. 37.5(a) are the efficiency-corrected (but not branching ratio corrected) CLEO and ARGUS inclusive cross sections, $s \cdot \mathcal{B} d\sigma/dx_p$, for the production of D^0 and D^{*+}. The variable x_p approximates the light-cone momentum fraction z in Eq. (37.9), but is not identical to it.

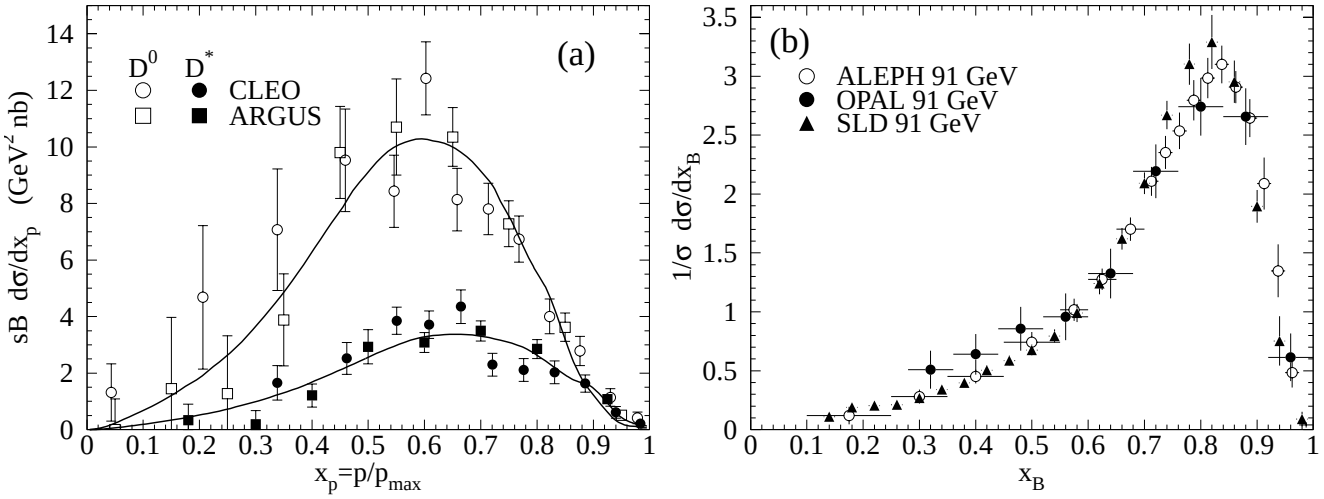

Figure 37.5: (a) Efficiency-corrected inclusive cross-section measurements for the production of D^0 and D^{*+} in e^+e^- measurements at $\sqrt{s} \approx 10$ GeV [35,40]. (b) Measured e^+e^- fragmentation function of b quarks into B hadrons at $\sqrt{s} \approx 91$ GeV [41,42].

For the D^0, $\mathcal{B}$ represents the product branching fraction: $D^{*+} \to D^0\pi^+$, $D^0 \to K^-\pi^+$. These inclusive spectra have not been corrected for cascades from higher states, nor for radiative effects. Since the momentum spectra are sensitive to QED and QCD radiative corrections, charm spectra at $\sqrt{s} = 10$ GeV cannot be compared directly with spectra at higher c.m. energies, and must be appropriately evolved. Tuning ϵ of (37.9) in the JETSET 7.4 Monte Carlo generator [17] using the parameter set of Ref. 20 and including radiative corrections to describe the combined CLEO and ARGUS D^0 and D^{*+} data gives $\epsilon_c = 0.043 \pm 0.004$; this is indicated in the solid curves.[2]

Experimental studies of the fragmentation function for b quarks, shown in Fig. 37.5(b), have been performed at LEP and SLD [36,41,42]. Commonly used methods identify the B meson through its semileptonic decay or based upon tracks emerging from the B secondary vertex. The most recent studies [42] fit the B spectrum using a Monte Carlo shower model supplemented with non-perturbative fragmentation functions yielding consistent results.

[2] This paragraph is adapted from D. Besson's contribution to C. Caso *et al.*, Eur. Phys. J. **C3**, 1 (1998).

The experiments measure primarily the spectrum of B mesons. This defines a fragmentation function which includes the effect of the decay of higher mass excitations, like the B^* and B^{**}. In the literature there is sometimes ambiguity in what is defined to be the bottom fragmentation function. Instead of using what is directly measured (*i.e.*, the B meson spectrum) corrections are applied to account for B^* or B^{**} production in some cases. For a more detailed discussion see Ref. 1.

Besides degrading the fragmentation function by gluon radiation, QCD evolution can also generate soft heavy quarks, increasing in the small x region as s increases. Several theoretical studies are available on the issue of how often $b\overline{b}$ or $c\overline{c}$ pairs are produced indirectly, via a gluon splitting mechanism [43–45]. Experimental results from studies on charm production via gluon splitting [46,47], and measurements of $g \to b\overline{b}$ [48–50] are given in Table 37.1.

Table 37.1: Measured fraction of events containing $g \to c\overline{c}$ and $g \to b\overline{b}$ subprocesses in Z decays, compared with theoretical predictions. The central/lower/upper values for the theoretical predictions are obtained with $m_c = (1.5 \pm 0.3)$ and $m_b = (4.75 \pm 0.25)\,\mathrm{GeV}$.

	$\overline{n}_{g\to c\overline{c}}$ (%)	$\overline{n}_{g\to b\overline{b}}$ (%)
OPAL	[46] $3.20 \pm 0.21 \pm 0.38$	
ALEPH	[47] $2.65 \pm 0.74 \pm 0.51$	[49] $0.277 \pm 0.042 \pm 0.057$
DELPHI		[48] $0.21 \pm 0.11 \pm 0.09$
SLD		[50] $0.307 \pm 0.071 \pm 0.066$
Theory [44]		
$\Lambda^{(5)}_{\overline{\mathrm{MS}}} = 150\,\mathrm{MeV}$	$1.35^{+0.48}_{-0.30}$	0.20 ± 0.02
$\Lambda^{(5)}_{\overline{\mathrm{MS}}} = 300\,\mathrm{MeV}$	$1.85^{+0.69}_{-0.44}$	0.26 ± 0.03

In Ref. 44 an explicit calculation of these quantities has been performed. Using these results, charm and bottom multiplicities as reported in Table 37.1 for different values of the masses and of $\Lambda^{(5)}_{\overline{\mathrm{MS}}}$ were computed in Ref. 51. The averaged experimental result for charm, $(3.10 \pm 0.34)\%$, is 1–2 standard deviations above the theoretical prediction, preferring lower values of the quark mass and/or a larger value of $\Lambda^{(5)}_{\overline{\mathrm{MS}}}$. However, higher-order corrections may well be substantial at the charm quark mass scale. Better agreement is achieved for bottom.

As reported in Ref. 44, Monte Carlo models are in qualitative agreement with these results, although the spread of the values they obtain is somewhat larger than the theoretical error estimated by the direct calculation. In particular, for charm one finds that while HERWIG [19] and JETSET [17] agree quite well with the theoretical calculation, ARIADNE [52] is higher by roughly a factor of 2, and thus is in better

agreement with data. For bottom, agreement between theory, models and data is adequate. For a detailed discussion see Ref. 53.

The discrepancy with the charm prediction may be due to experimental cuts forcing the final state configuration to be more 3-jet like, which increases the charm multiplicity. Calculations that take this possibility into account are given in Ref. 45.

References:

1. O. Biebel, P. Nason, and B.R. Webber, Bicocca-FT-01-20, Cavendish-HEP-01/12, MPI-PhE/2001-14, `hep-ph/`0109282.
2. L.N. Lipatov, Sov. J. Nucl. Phys. **20**, 95 (1975);
   V.N. Gribov and L.N. Lipatov, Sov. J. Nucl. Phys. **15**, 438 (1972);
   G. Altarelli and G. Parisi, Nucl. Phys. **B126**, 298 (1977);
   Yu.L. Dokshitzer, Sov. Phys. JETP **46**, 641 (1977).
3. P. Nason and B.R. Webber, Nucl. Phys. **B421**, 473 (1994); erratum *ibid.*; **B480**, 755 (1996).
4. W. Furmanski and R. Petronzio, preprint TH.2933–CERN (1980), Phys. Lett. **97B**, 437 (1980).
5. R.K. Ellis, J. Stirling, and B.R. Webber: *QCD and Collider Physics*, Cambridge University Press, Cambridge (1996).
6. TASSO Collaboration: R. Brandelik *et al.*, Phys. Lett. **B114**, 65 (1982);
   W. Braunschweig *et al.*, Z. Phys. **C47**, 187 (1990);
   HRS Collaboration: D.Bender *et al.*, Phys. Rev. **D31**, 1 (1984);
   MARK II Collaboration: A. Petersen *et al.*, Phys. Rev. **D37**, 1 (1988);
   AMY Collaboration: Y.K. Li *et al.*, Phys. Rev. **D41**, 2675 (1990);
   ALEPH Collaboration: D. Buskulic *et al.*, Z. Phys. **C73**, 409 (1997);
   OPAL Collaboration: R. Akers *et al.*, Z. Phys. **C72**, 191 (1996);
   K. Ackerstaff *et al.*, Z. Phys. **C75**, 193 (1997);
   G. Abbiendi *et al.*, Eur. Phys. J. **C16**, 185 (2000).
7. TPC Collaboration: H. Aihara *et al.*, Phys. Rev. Lett. **61**, 1263 (1988).
8. DELPHI Collaboration: P. Abreu *et al.*, Eur. Phys. J. **C6**, 19 (1999).
9. ALEPH Collaboration: E. Barate *et al.*, Phys. Reports **294**, 1 (1998);
   L3 Collaboration: B. Adeva *et al.*, Phys. Lett. **B259**, 199 (1991);
   OPAL Collaboration: K. Ackerstaff *et al.*, Eur. Phys. J. **C7**, 369 (1998);
   MARK II Collaboration: G.S. Abrams *et al.*, Phys. Rev. Lett. **64**, 1334 (1990).
10. DELPHI Collaboration: P. Abreu *et al.*, Phys. Lett. **B398**, 194 (1997).
11. ALEPH Collaboration: D. Barate *et al.*, Phys. Lett. **B357**, 487 (1995); erratum *ibid.*; **B364**, 247 (1995).
12. DELPHI Collaboration: P. Abreu *et al.*, Eur. Phys. J. **C13**, 573 (2000); Phys. Lett. **B311**, 408 (1993);

W. de Boer and T. Kußmaul, IEKP-KA/93-8, hep-ph/9309280;;
B.A. Kniehl, G. Kramer, and B. Pötter, Phys. Rev. Lett. **85**, 5288 (2001).

13. OPAL Collaboration: R. Akers *et al.*, Z. Phys. **C86**, 203 (1995).
14. ALEPH Collaboration: R. Barate *et al.*, Eur. Phys. J. **C17**, 1 (2000);
OPAL Collaboration: G. Abbiendi *et al.*, Eur. Phys. J. **C11**, 217 (1999);
R. Akers *et al.*, Z. Phys. **C68**, 179 (1995).
15. X. Artru and G. Mennessier, Nucl. Phys. **B70**, 93 (1974).
16. B. Andersson, G. Gustafson, G. Ingelman, T. Sjöstrand, Phys. Reports **97**, 31 (1983).
17. T. Sjöstrand and M. Bengtsson, Comp. Phys. Comm. **43**, 367 (1987);
T. Sjöstrand, Comp. Phys. Comm. **82**, 74 (1994).
18. S. Chun and C. Buchanan, Phys. Reports **292**, 239 (1998).
19. G. Marchesini *et al.*, Comp. Phys. Comm. **67**, 465 (1992);
G. Corcella *et al.*, JHEP **0101**, 010 (2001).
20. OPAL Collaboration: G. Alexander *et al.*, Z. Phys. **C69**, 543 (1996).
21. M. Schmelling, Phys. Scripta **51**, 683 (1995).
22. D. Amati and G. Veneziano, Phys. Lett. **B83**, 87 (1979).
23. ALEPH Collaboration: D. Buskulic *et al.*, Z. Phys. **C66**, 355 (1995);
ARGUS Collaboration: H. Albrecht *et al.*, Z. Phys. **C44**, 547 (1989);
DELPHI Collaboration: P. Abreu *et al.*, Eur. Phys. J. **C5**, 585 (1998);
OPAL Collaboration: R. Akers *et al.*, Z. Phys. **C63**, 181 (1994);
SLD Collaboration: K. Abe *et al.*, Phys. Rev. **D59**, 052001 (1999).
24. B.A. Kniehl, G. Kramer and B. Pötter, Nucl. Phys. **B597**, 337 (2001).
25. L. Bourhis *et al.*, Eur. Phys. J. **C19**, 89 (2001);
B.A. Kniehl, G. Kramer, and B. Pötter, Nucl. Phys. **B582**, 514 (2000);
J. Binnewies, B.A. Kniehl, and G. Kramer, Phys. Rev. **D52**, 4947 (1995);
Z. Phys. **C65**, 471 (1995);
J. Binnewies, Hamburg University PhD Thesis, DESY 97-128, hep-ph/9707269.
26. V.A. Khoze, Ya.I. Azimov, and L.L. Frankfurt, Proceedings, Conference on High Energy Physics, Tbilisi 1976;
J.D. Bjorken, Phys. Rev. **D17**, 171 (1978).
27. B. Mele and P. Nason, Phys. Lett. **B245**, 635 (1990); Nucl. Phys. **B361**, 626 (1991).
28. Y. Dokshitzer, V.A. Khoze, and S.I. Troyan, Phys. Rev. **D53**, 89 (1996).
29. M. Cacciari and S. Catani, CERN-TH/2001-174, UPRF-2001-11, hep-ph/0107138.
30. P. Nason and C. Oleari, Phys. Lett. **B418**, 199 (1998) *ibid.*; **B447**, 327 (1999); Nucl. Phys. **B565**, 245 (2000).
31. C. Peterson *et al.*, Phys. Rev. **D27**, 105 (1983).

32. V.G. Kartvelishvili, A.K. Likehoded, and V.A. Petrov, Phys. Lett. **B78**, 615 (1978).
33. P. Collins and T. Spiller, J. Phys. **G11**, 1289 (1985).
34. OPAL Collaboration: R. Akers *et al.*, Z. Phys. **C67**, 27 (1995).
35. ARGUS Collaboration: H. Albrecht *et al.*, Z. Phys. **C52**, 353 (1991).
36. ALEPH Collaboration: D. Buskulic *et al.*, Phys. Lett. **B357**, 699 (1995).
37. J. Chrin, Z. Phys. **C36**, 163 (1987).
38. R.L. Jaffe and L. Randall, Nucl. Phys. **B412**, 79 (1994);
    P. Nason and B. Webber, Phys. Lett. **B395**, 355 (1997).
39. G. Colangelo and P. Nason, Phys. Lett. **B285**, 167 (1992);
    L. Randall and N. Rius, Nucl. Phys. **B441**, 167 (1995).
40. CLEO Collaborations: D. Bortoletto *et al.*, Phys. Rev. **D37**, 1719 (1988).
41. OPAL Collaboration: G. Alexander *et al.*, Phys. Lett. **B364**, 93 (1995);
    L3 Collaboration: B. Adeva *et al.*, Phys. Lett. **B261**, 177 (1991).
42. SLD Collaboration: K. Abe *et al.*, Phys. Rev. Lett. **84**, 4300 (2000);
    ALEPH Collaboration: A. Heister *et al.*, Phys. Lett. **B512**, 30 (2001).
43. A.H. Mueller and P. Nason, Nucl. Phys. **B266**, 265 (1986);
    M.L. Mangano and P. Nason, Phys. Lett. **B285**, 160 (1992).
44. M.H. Seymour, Nucl. Phys. **B436**, 163 (1995).
45. D.J. Miller and M.H. Seymour, Phys. Lett. **B435**, 213 (1998).
46. OPAL Collaboration: G. Abbiendi *et al.*, Eur. Phys. J. **C13**, 1 (2000).
47. ALEPH Collaboration: R. Barate *et al.*, Eur. Phys. J. **C16**, 597 (2000).
48. DELPHI Collaboration: P. Abreu *et al.*, Phys. Lett. **B405**, 202 (1997).
49. ALEPH Collaboration: R. Barate *et al.*, Phys. Lett. **B434**, 437 (1998).
50. SLD Collaboration: K. Abe *et al.*, SLAC-PUB-8157, `hep-ex/9908028`.
51. S. Frixione, M.L. Mangano, P. Nason, and G. Ridolfi: Heavy Quark Production, in A.J. Buras and M. Lindner (eds.), *Heavy Flavours II*, World Scientific, Singapore (1998), `hep-ph/9702287`.
52. L. Lönnblad, Comp. Phys. Comm. **71**, 15 (1992).
53. A. Ballestrero *et al.*, CERN-2000-09-B, `hep-ph/0006259`.